ARTICLES

Relaxation Dynamics of Naphthalene and 1-Aminonaphthalene in Superexcited States

Raúl Montero, Fernando Castaño,* Roberto Martínez, and Asier Longarte

Departamento de Química-Física, Facultad de Ciencia y Tecnología, Universidad del País Vasco. Apart. 644, 48080 Bilbao, Spain

Received: June 25, 2008; Revised Manuscript Received: October 9, 2008

The relaxation dynamics of naphthalene (NPH) and 1-aminonaphthalene (AMN) in superexcited (SE) states has been investigated by pump−probe femtosecond ionization. SE states were produced by two-photon resonant absorption via S_1 and S_2 states and their time evolution probed by ionization with 800 nm light pulses. A fine-tuning of the pump and probe laser intensities permits us to separate the dynamics of the SE states from that of the S_1/S_2 intermediate states. SE state relaxation pathways were investigated in the channels of the parent and the major fragment ions. The lifetimes of two relaxation processes were derived from the exponential fit and found to be in the femtosecond and the picosecond time scales. The fast component is attributed to internal conversion (IC) from the SE states to the Rydberg states, whereas the slow one, only observed in the fragment transients, is assigned to fragmentation of the relaxed neutral molecules. The study sheds light on the significant role of SE states dynamics in pump−probe ionization experiments.

Introduction

The study of large polyatomic molecules in excited states near and even above the first ionization potential (IP) − known as superexcited (SE) states −[1] has attracted considerable attention in recent years. The complex nature of the states and the large variety of photophysical and photochemical phenomena in which they are involved make the experimental and theoretical research a challenging task. On the other hand, molecules in high excited states are a major source of information on molecular structure and fundamental processes, such as ionization, charge and energy transfer, and reactivity, where they play a crucial role.

High-density laser radiation of appropriate wavelength absorbed by a molecule AB yields (among others) highly excited species, including ions, ionic fragments, and SE states, as indicated below:

$$\begin{aligned} AB + h\upsilon &\rightarrow AB^+ + e^- && \text{direct ionization} \\ &\rightarrow A^+ + B + e^- && \text{ion fragmentation} \\ &\rightarrow AB^{**} && \text{SE state formation} \end{aligned}$$

Relaxation of the SE state (AB**) is commonly accepted to take place by a number of channels, being the most relevant:

$$\begin{aligned} AB^{**} &\rightarrow AB^+ + e^- && \text{autoionization} \\ &\rightarrow (AB)^* && \text{electronic relaxation} \\ &\rightarrow A^* + B && \text{neutral fragmentation} \end{aligned}$$

The participation of SE states in ionization and neutral dissociation has been the subject of a number of works employing a variety of experimental methods. Among them, the studies on Rydberg SE states of diatomic or small polyatomic molecules have been the most abundant.[2] Because of the high energy required to reach SE states, only techniques such as VUV radiation, UV−vis multiphoton absorption, and electron impact have been used to prepare them, whereas the characterization has been frequently carried out by photoion or photoelectron detection.[2] The development of delayed ion/electron extraction techniques (e.g., ZEKE/MATI spectroscopies) has provided access to SE states of high stability placed just on the top of Rydberg series converging to ion states. These new methods have been successfully applied to large polyatomic molecules[3] and permitted the identification of long-lived SE states in a range of few eVs above the first IP.[4]

The appearance of ultrashort and intense laser pulses has made a powerful tool available to study SE states in two key facets: producing a large density of highly excited atoms or molecules by multiphoton absorption and providing the time resolution to study the evolution of the SE states. Femtosecond pulses have been applied to investigate the dynamics of SE states in a reduced number of polyatomic molecules.[5−8] The observed decays have lifetimes in the femto- and pico-second regimes and give significant information on the role played by these states in ionization, ion fragmentation, and molecular reactivity.

The present study uses femtosecond sources to investigate the dynamics of excited states with energies above the first IP in the naphthalene (NPH) and 1-aminonaphthalene (AMN) molecules. Because of the low IP of the NPH chromophore (8.14 eV), the SE states can be accessed by absorption of two near-UV photons. The excitation was carried out at a number of wavelengths involving the resonant absorption of two quanta through either S_1 or S_2 intermediate electronic states. Further probing is accomplished by single or multiphoton ionization with 800 nm probe pulses. Fine-tuning of individual pump and probe beam intensities permits one to distinguish the contribution of the SE states from that of the S_1/S_2 states.[9] We have followed the time-evolution of the SE states by recording the transient of the parent ion and some ion fragments produced in the ionization process. At the excitation wavelengths studied, the collected transients provide evidence on the efficient formation of SE states and their competition with prompt ionization. The

* To whom correspondence should be addressed: E-mail: f.castano@ehu.es. Fax: ++ 34 94 464 85 00. Phone ++ 34 94 601 2533.

10.1021/jp8056064 CCC: $40.75
Published on Web 01/20/2009

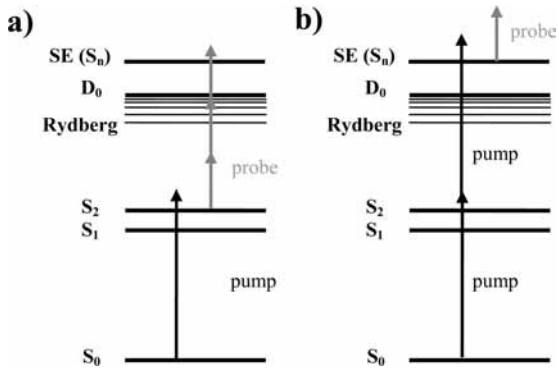

Figure 1. (a) $1 + 3'$ transient ionization scheme to access the dynamics of the S_2/S_1 excited states. (b) $2 + 1'$ scheme to monitor the SE state dynamics. The electronic and vibrational energy content of the created ions is expected to be the different in both cases.

set of SE states relaxes along a complex pathway that includes at least two components, with lifetimes in the femto- and picosecond time scales. The time evolution of the system is understood on the grounds of a kinetic model that involves internal conversion (IC) to nearby Rydberg states, followed by fragmentation induced by internal vibrational redistribution of the relaxed electronic energy. The present work also addresses the role of SE states in multiphoton ionization processes with intense laser pulses.

Experimental Section

The ionization schemes shown in Figure 1 have been alternatively used to access the SE or the S_1/S_2 states dynamics. Part a of Figure 1 depicts the absorption of a single photon from a low-intensity pump laser to yield S_1 or S_2 vibronic states, followed by ionization of the emerging state with 800 nm photons, in a $1 + 3'$ ionization process. In part b of Figure 1, the SE (S_n) state is reached by the absorption of two pump photons and further ionized by a lower intensity probe laser, according to a $2 + 1'$ ionization scheme. The scheme of part a of Figure 1 allows monitoring the relaxation of the S_1/S_2 states, whereas that of part b of Figure 1 tracks the dynamics of the SE state. In consequence, an appropriate tuning of pump and probe laser intensities allows the separation of their dynamics.

Setup. NPH and AMN transients were recorded using a pump−probe set up with ion-mass resolved detection.[10] The chemicals, purchased from Aldrich and used without purification, were heated up to 80 °C, seeded in Ar at a stagnation pressure of 1−2 atm, and further expanded through the 0.5 mm ϕ nozzle of an electromagnetic pulsed valve (General Valve) into a vacuum chamber at a pressure of $\sim 10^{-6}$ mbar. A small portion of the molecular beam plume is collimated by a skimmer before passing to the ionization region of a linear time-of-flight spectrometer, where it interacts with the pump−probe laser pulses. The resulting ions are further accelerated by circular plates set at appropriate voltages that send them along the axis of the TOF tube to the 18 mm dual MCP detector.

Ultrashort light pulses were generated by a commercial Ti:sapphire oscillator-regenerative amplifier laser system (Coherent) that provides a 1 kHz train of 40 fs pulses centered at 800 nm. A portion of the amplifier output drives either an optical parametric amplifier (OPA) tunable in the 300−2600 nm range (Coherent OPERA) or a third harmonic generator (267 nm) being used as pump beams at convenience. Another fraction of the amplifier output beam (800 nm) is sent to the spectrometer to probe the molecules by single or multiphoton ionization. The delay between pump and probe pulses is controlled by the displacement of a retroreflector mirror with a total equivalent travel of 150 ps. The laser beams were send to the TOF mass spectrometer almost collinearly, with an angle smaller than 5°, and focused maximizing the resulting ion signal. Pump and probe intensities were controlled using gradient neutral density filters. For the power dependence measurements, intensities in the ranges 10^9-10^{10} W/cm^2 and $10^{10}-10^{11}$ W/cm^2 were employed for pump and probe, respectively. The linearly polarized beams were kept at the magic angle configuration (54.7° between the polarization planes).

The mass spectrum was monitored with a digital oscilloscope and the ion signal of selected masses (up to a maximum of three) integrated with boxcar integrators (Stanford SR250) for each valve pulse. The dc voltage output of the boxcar was synchronously acquired with that of the pump−probe delay via an A/D converter (National Instruments) and stored in a PC computer for analysis. The repetition rate of the pulsed valve was limited by the pumping capacity of the system and kept in the 100−200 Hz range. A delay generator (Stanford DG535) takes the 1 kHz reference signal from the laser and divides it by a variable factor to fire the valve. A total of 3×10^5 shots were usually accumulated in one scan, providing an average of 3×10^3 points for each selected delay time.

To provide the accurate zero delay time and the pump−probe cross correlation function the nonresonant ionization signal of ethylene ($1 + 4'$) was recorded along with the signals of interest. From the cross-correlation, the pump and probe pulse widths (fwhm) have been determined to be 110−180 fs (wavelength dependent) and 60 fs respectively.

Kinetic Model. The kinetic model employed to fit the transients of NPH and AMN excited states includes, in addition to decay processes, the influence of the resonant two-photon excitation that yields the SE states. A sketch of the model is shown in part a of Figure 2, where f_{ab}, f_{ba} and f_{bc}, f_{cb} are the fraction of molecules excited or induced to emit (saturation effect);[11] k_b and k_c are the relaxation rate constants of the resonant intermediate ($|b\rangle$) and the SE ($|c\rangle$) states, respectively. The linear differential equations describing the model were numerically solved by the Runge−Kutta method implemented in the *Mathematica* package.[12] Part b of Figure 2 analyzes the influence of a long-lived intermediate state and the saturation effect over the formation of a hypothetical stationary SE state, in contrast with a nonresonant nonsaturated two-photon excitation (solid line in part b of Figure 2). For a resonant excitation in a nonsaturated regime (dotted line), the S_n state reaches half of the system's total population at positive times ($t = 0$ being the maximum of the Gaussian function that describes the pump pulse). If saturation of the intermediate state is included in the model (dashed line), the positive time shift is corrected and the half-maximum population is reached near time zero, which is the expected behavior in a nonresonant nonsaturated excitation process.[11] We have considered the saturation of the resonant step in the fittings of NPH and AMN at all of the excitation wavelengths.

The dynamics of the resonant intermediate state also affects the population of the SE state when its rate constant is comparable to the fwhm of the pump pulse. Part c of Figure 2 shows the time evolution of a hypothetical S_n state with a lifetime k_c^{-1} equal to the pump pulse fwhm. Three limit cases of rate constant k_b have been explored, namely $k_b \ll 1/\text{fwhm}$, $k_b = 1/\text{fwhm}$, and $k_b = 10/\text{fwhm}$. For resonant intermediate states with a relaxation time shorter than the pump pulse, the transient rising and decaying wings of the S_n state are

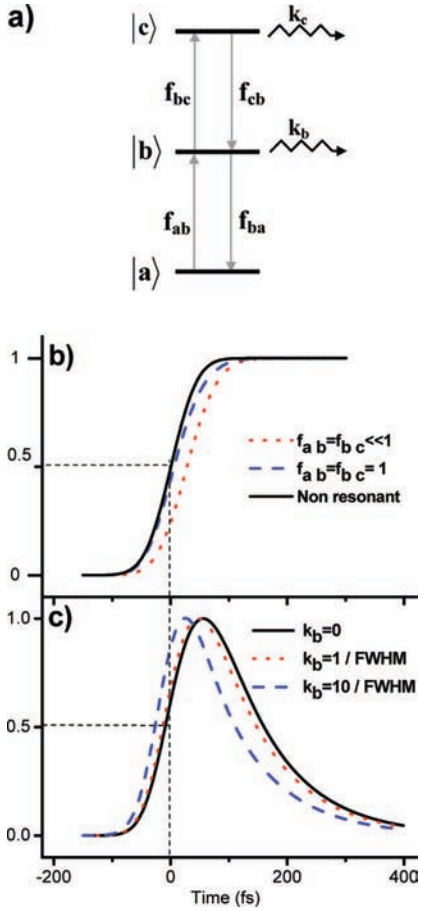

Figure 2. (a) Scheme of the three level kinetic model used to fit the transients of the SE state ($|c\rangle$) dynamics. f_{ab}, f_{ba} and f_{bc}, f_{cb} stand for the fraction of molecules excited or induced to emit by the pump pulse and are proportional to the transition probability times the radiation density. k_b and k_c are the relaxation rate constants to deplete the populations of the $|b\rangle$ and $|c\rangle$ states, respectively. f_{ab}, f_{bc}, and k_b control the growth of the SE state population and k_c its depletion. The probing process is not included in the scheme. (b) Effect of pump saturation on the SE population compared to a nonresonant nonsaturated pumping process (text for details). (c) Effect on the SE population of the resonant excitation step dynamics (text for details).

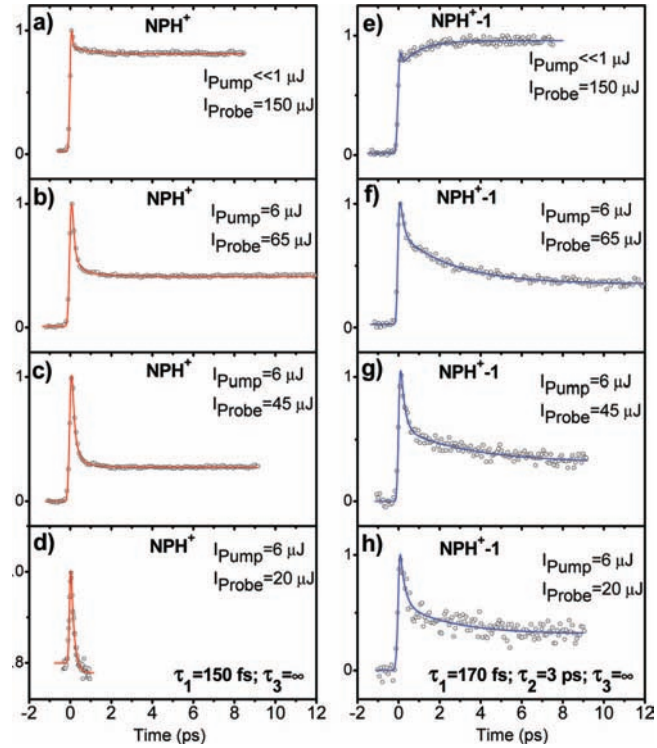

Figure 3. Transient ion signals recorded with 267 nm excitation and 800 nm probe in the $C_{10}H_8^+$ (a−d) and $C_{10}H_7^+$ (e−h) ion mass channels. Dots are the experimental data and solid lines are their best obtained fits. Traces a and e were collected at low pump energy and reproduce the dynamics of the NPH S_2 state. In decays d and h, the lifetimes of the SE state have been isolated by keeping high pump and low probe intensity. The other traces correspond to intermediate intensities and then a mixture of the S_2 and SE state dynamics is found. The vertical scales are referred to the absolute zero ion current (text). In b and c traces, the pump background has been subtracted from the measured signal.

significantly affected. In the present work, the influence of the intermediate state dynamics in the NPH and AMN SE state transients excited at 267 nm has been observed. In NPH, the 30 fs lifetime required for a good fit of the rising part of the transient is related to ultrafast relaxation of S_2 during the excitation. In the gas phase, the S_2 state lays 0.5 eVs above S_1 and their strong coupling favors the ultrafast IC that shortens its lifetime to 30 fs.[8b,9] The formation of the SE state via the S_1 populated from the relaxed S_2 is much less efficient than the direct excitation through S_2, causing the observed shift of the transient to negative delay times. For AMN excited at 267 nm, we have measured a S_2 lifetime of 110 fs[13] that has also been used to fit the rising part of the transient.

Results

Naphthalene. Figure 3 displays a set of transients collected at the parent $C_{10}H_8^+$ and the $C_{10}H_7^+$ fragment ion channels following absorption of 267 nm photons (via S_2 state) and further probing with 800 nm laser pulses. Fragmentation takes place in the ions created in the probe process and thus the transients collected in the fragment channel include dynamic information on the neutral species (Discussion for further details). A comprehensive discussion on the fragmentation produced by probing photons in ionization experiments is presented in ref 14.

In the transients 3a and 3e, the pump energy was kept as low as 0.1 μJ, whereas the probe energy was ~150 μJ. The low pump intensity hampers ionization in the absence of the probe pulse, suggesting a single photon absorption process. Hence, traces 3a and 3e reflect the time evolution of NPH S_2 state, according to the pump−probe scheme of part a of Figure 1. This dynamics will be the subject of a forthcoming article.[9] Along 3a−d and 3e−h plot sequences, the probe intensity was diminished according to the value detailed in each graph, whereas the pump energy was kept high enough to induce a two-photon absorption. At these intensities, transients 3b and 3c of the parent contain contributions from the S_2 and the SE states, as revealed by the time constants derived from these decays. Traces 3d of the parent and 3f−h of the fragment are cases where ionization from the S_1/S_2 states is negligible and hence they correspond to the dynamics of the SE state.

To shed light on the nature of the dynamics observed in the transients, a series of power-dependent measurements of both parent and fragment ion signals were carried out for NPH and AMN (not shown). Figure 4 shows a double logarithm plot of the parent ion current versus the pump beam intensity, with the probe laser off and on. Both sets of data were collected at identical pump intensities and with a 30 fs pump−probe delay in the latter. The fittings to straight lines yield slopes >1.0, the expected values for a two-photon absorption process through a

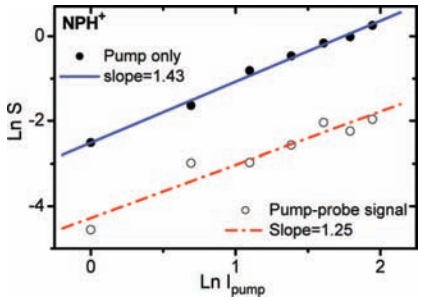

Figure 4. Double logarithmic plot of the NPH^+ parent ion signal versus pump intensity along with the best obtained linear fit. The black dots and the solid line correspond to the ion current induced by the pump only, whereas the circles and the dashed line to the pump−probe signal at 30 fs delay. In the latter, the probe energy was kept around 50 μJ and the background signal generated by the pump was subtracted.

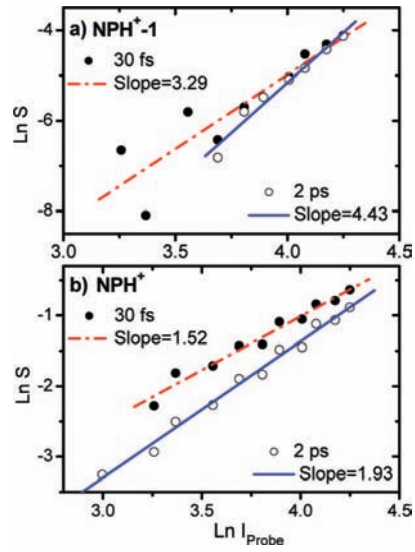

Figure 5. Double logarithmic plot of the $(NPH\text{-}1)^+$ fragment (a) and NPH^+ (b) parent ion signals versus the probe beam intensity, at low pump energy (<0.1 μJ). At these conditions, ions are formed by absorption of the probe on the S_2/S_1 states. The experimental data and the best linear fits are plotted for two selected pump−probe delays.

resonant intermediate state.[15] Similar logarithmic plots of the parent and fragment ion signal versus probe intensity are shown in Figures 5 and 6 at short (30 fs) and long (2 ps) delay times. The measurements plotted in Figure 5 were carried out keeping the laser pump energy low enough to ensure a negligible background in the parent and fragment channels, and thus one concludes that the ions are created by absorption of probe photons from the S_2/S_1 intermediate states. On the contrary, in Figure 6 the pump laser intensity was increased to yield ~20% of the total ion current in the parent ion mass channel, allowing the excitation to SE states. The detailed analysis of these data is presented below.

Figure 7 displays the transients of the parent NPH^+ and the $C_{10}H_7^+$ fragment ions excited at 304 nm (4.08 eV), along with the best exponential fits. The wavelength is resonant with the quasi-forbidden $S_1 \leftarrow S_0$ transition[16] and the absorption of two photons promotes the system to an SE state nearby the first IP (8.14 eV). The decays were collected after optimizing the pump and probe intensities to isolate the SE state dynamics.

The time constants and ionization cross sections (associated with the relaxation of the SE state) derived from the fits of NPH^+ and $C_{10}H_7^+$ transients excited at 267 and 304 nm are collected in Table 1. Note that whereas the parent ion decays have a single

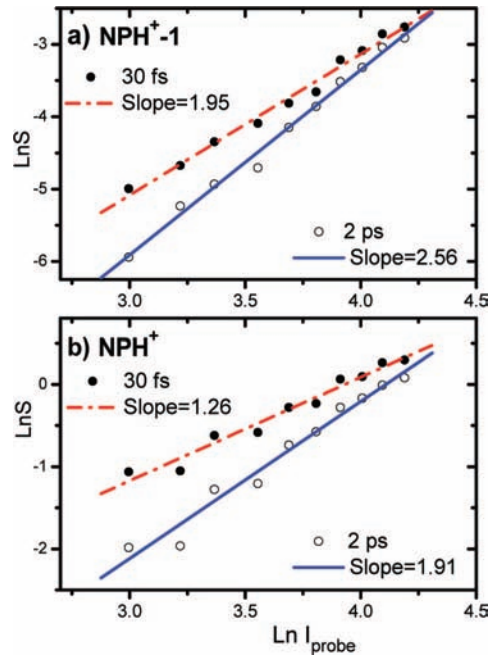

Figure 6. Double logarithmic plot of the $(NPH\text{-}1)^+$ fragment (a) and NPH^+ parent ion (b) signals versus the probe beam intensity, at high pump energy (3 μJ). Data were collected at 50 fs and 2 ps pump−probe time delays.

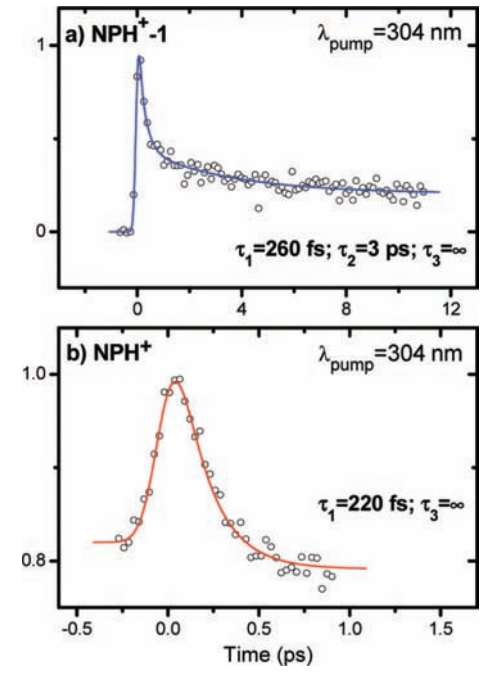

Figure 7. Transient ion signals of the $(NPH\text{-}1)^+$ fragment (a) and NPH^+ parent ion (b), recorded via S_1 resonant excitation at 304 nm. Pump and probe intensities were adjusted to isolate the dynamics of the SE state. The fitting of NPH^+ parent ion decay required an additional $1 + 3'$ nonresonant component. The vertical scales are referred to the absolute zero ion current (text).

femtosecond lifetime, the fragments show a double exponential with an additional picosecond component.

1-Aminonaphthalene. SE states of AMN were prepared by two-photon absorption at 333, 300, and 267 nm and further probing in all cases by ionization with 800 nm laser pulses. The excitation wavelengths are resonant with the S_1/S_2 manifold, and the absorption of two quanta promotes the system to states with an energy increment over the vertical IP of −0.04, 0.79,

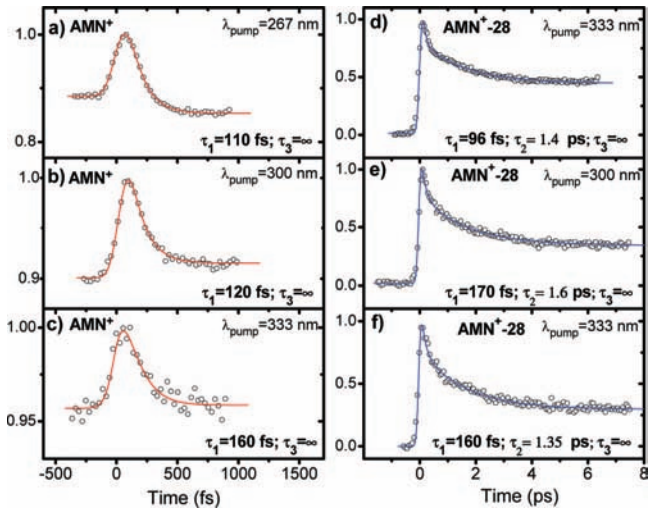

Figure 8. Transients measured in the AMN^+ (a−c) and AMN^+-28 mass channels (d−f), at the pump laser wavelengths: 267nm (a, d), 300nm (b, e), and 333 nm (c, f). Pump and probe laser intensities were tuned to favor the $2 + 1'$ ionization, to separate the dynamics of the SE states. However, the offset observed at positive times in b and c points out the presence of a small contribution from the lower S_2/S_1 excited states. The vertical scales are referred to the absolute zero ion current (text).

and 1.81 eV, respectively. Analogously to NPH, an analysis on the dependence of the ion signal on the pump and probe intensities was carried out for AMN (not shown) to avoid contamination from the dynamics of lower excited states. Figure 8 shows the transients of the AMN^+ parent ion and the major fragment observed in the mass spectrum, AMN^+-28 amu. The lifetimes derived from the exponential fits are indicated in the figure and summarized in Table 2 along with the ionization cross sections.

Discussion

Formation of Superexcited States. Let us begin by analyzing the ability of the experiment to form SE states and isolate their dynamics. Both NPH and AMN molecules have between the first excited electronic state and the IP an energy gap large enough to hamper the preparation of SE states by nonresonant two-photon excitation. Use of S_1 or S_2 states as intermediate resonant steps provides an efficient method to create highly excited species but in turn introduces the contribution of the intermediate state dynamics. In consequence, the correlation between the ion signal and the pump and probe laser intensities is crucial to track the origin of the observed transients. Figure 4 depicts the relationship between the NPH^+ ion signal and the pump laser intensity with either the probe laser off or on. The slope of the best linear fit is 1.44 with the probe laser off and 1.25 (pump background subtracted) if it is on. Bearing in mind that the models predict a slope <2 for two-photon REMPI processes,[15] and that the slope of the pump-only is 1.44 and diminished to 1.25 in with the probe on, it is concluded that most of the signal comes from the ionization of SE states produced by absorption of two pump photons.

The dependence of the parent and fragment ion signals on the probe laser intensity substantiates the selectivity of the experiments to track the SE state dynamics. The comparison of the NPH^+ short time data of Figures 5 and 6 shows a decrease in the slope from 1.52 to 1.26, in contrast with long time results (2 ps) where the slopes remain almost constant around 1.9. This change is associated with the contribution of the $2 + 1'$ ionization at high pump intensities, which at short times produces a decrease in the probe dependence with respect to the $1 + 3'$ absorption. Note that the $2 + 1'$ signal decays in the femtosecond time scale, and hence at 2 ps the ion current comes from the $1 + 3'$ absorption and the slope of the probe dependence does not change with the pump intensity, as stated above.

TABLE 1: Lifetimes (τ_i) and Ionization Cross Sections (s_i) of the SE and Rydberg States Considered in the Kinetic Model extracted from the Exponential Fits of the NPH^+ and NPH^+-1 Transients[a]

		s_1	τ_1	s_2	τ_2	a_3[b]	τ_3
267 mn	NPH^+	1	150 ± 20 fs			−0.09	∞
	NPH^+-1	1	170 ± 20 fs	0.25	3 ± 0.5 ps	0.24	∞
304 mn	NPH^+	1	220 ± 30 fs			−0.02	∞
	NPH^+-1	1	260 ± 50 fs	0.27	3.5 ± 0.5 ps	0.26	∞

[a] The error bars are the standard deviations computed from five scans. [b] a_3 is the coefficient of a $\tau = \infty$ component added the solution of the kinetic model to account for the background observed at positive times.

TABLE 2: Lifetimes (τ_i) and Ionization Cross Sections (s_i) of the SE and Rydberg States Considered in the Kinetic Model Extracted from the Exponential Fits of the AMN^+ and AMN^+-28 Transients[a]

		s_1	τ_1	s_2	τ_2	a_3[b]	τ_3
267 mn	AMN^+	1	110 ± 10 fs			−0.1	∞
	AMN^+-28	1	96 ± 10 fs	0.25	1.4 ± 0.2 ps	0.26	∞
300 mn	AMN^+	1	120 ± 20 fs			0.09	∞
	AMN^+-28	1	170 ± 20 fs	0.48	1.6 ± 0.3 ps	0.29	∞
333 mn	AMN^+	1	160 ± 25 fs			0.1	∞
	AMN^+-28	1	160 ± 25 fs	0.42	1.35 ± 0.3 ps	0.39	∞

[a] The error bars are the standard deviations computed from five scans. [b] a_3 is the coefficient of a $\tau = \infty$ component added the solution of the kinetic model to account for the background observed at positive times.

The NPH^+-1 ion exhibits from Figure 5 to Figure 6 a change in probe intensity larger than that found for the parent ion. Indeed, the slopes at short and long times vary from 3.29 to 1.95 and from 4.43 to 2.56, respectively. In consequence, it is easier to isolate the dynamics of the SE state in the NPH^+-1 fragment ion. The conclusion is also supported by comparing traces in panels 3b and 3f. Whereas in the 3b the contribution of the S_1/S_2 states is still present, in similar conditions the fragment channel in panel 3f only reproduces the SE state dynamics.

The character of the created SE state is determined by the absorption process. For all the studied excitation wavelengths SE states of NPH and AMN are reached by a two-photon resonant absorption via the S_1 or S_2 state. Because of the small oscillator strength of the $S_1 \leftarrow S_0$ transition, a nonresonant contribution could be present when exciting via the S_1 state but is expected to be small. The electronic configurations of both neutral and ionized NPH in the ground and lowest excited states are well-known. The two coupled neutral excited states, S_1 (3.97 eV) and S_2 (4.45 eV), have contributions of two single excitations[16] and each of them correlates under Koopman's propensity rules, with the cation ground D_0 and first excited D_1 states.[8b] The absorption of two 267 nm photons (9.3 eV) through S_2 raises the NPH molecule over the D_1 ion state at 8.88 eV.[17] The first photon induces a $\pi_{ring} \rightarrow \pi_{ring}^*$ transition, whereas the second one inevitably promotes a different electron. Comparing the ionization background (prompt ions and autoionized molecules) produced by absorption of the pump laser with the

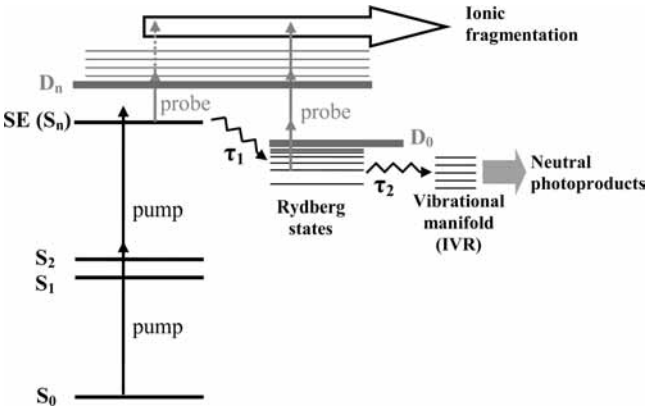

Figure 9. Scheme of the energy levels and channels proposed to be involved in the SE states formation and relaxation. Initial excitation by two pump photons is followed by ultrafast internal IC (τ_1) to nearby Rydberg levels. A second process in the picosecond scale (τ_2) is attributed to IVR and leads to the formation of neutral fragments. An additional $\tau_3 = \infty$ lifetime, associated to the fragmentation of the ions produced by direct or autoionization, has been used to fit the transients but is not shown in the plot.

pump−probe signal at $\Delta t = 0$ (cf. part b of Figure 7), the SE state formation emerges as an efficient process, induced by an $S_2 \rightarrow S_n$ transition with a significant oscillator strength. This observation suggests that the main contributors to the formation of the SE state are single electron excitations between S_2 and valence orbitals that fulfill energy and symmetry constrictions. Likewise, the SE state is also reached via S_1, but in this case the second photon in addition to a valence orbital could also excite the electron to a Rydberg state converging to the D_1 state of the cation, or even to the ground D_0 state with a small vibrational content. Therefore, the two-photon excitation of NPH via S_1 and S_2 likely prepares the molecule in an SE state or in a mixture of them that includes configurations resulting of double excitations involving valence states and even some excitations of Rydberg character. The excitation is even more complicated for AMN, where the relative energy of S_1 and S_2 states is not firmly established.[18,19] They are believed to lie very close in energy and to be strongly coupled,[20] thus, at the employed wavelengths, the excitation might take place simultaneously through both states.

Relaxation of Superexcited States. The decays of the parent and fragment ions contain the relaxation dynamics of the SE states. The model proposed to explain the processes involved is sketched in Figure 9 and applies to both studied molecules. The initially created SE state decays in the femtosecond time scale as reflected by the lifetime τ_1 extracted from the transients of the parent and the associated fragment ion. The presence of the lifetime τ_1 in both channels substantiates that the fragmentation takes place in the ion involving the absorption of additional probe photons. This statement is further validated by the measurements on the ion current as a function of the probe intensity (Figure 6). The steeper slope of the fragment ion at earlier times compared to that of the parent ions (1.95 vs 1.26) also evidences the absorption of additional photons to fragment. In fact, the heat of formation of $C_{10}H_7^+$ from NPH^+ is estimated to be 11.29 eV,[21] implying that following the 267 nm two-photon absorption (9.3 eV) at least two more 800 nm quanta are required to produce the fragment.

The photoelectron studies reported by Weber's group on NPH[22] and phenol[5a] grant a firm basis to recognize the nature of the observed femtosecond decay, τ_1. They identified the relaxation to Rydberg states as the primary deactivation channel of the SE sates. A similar relaxation mechanism has also been observed in amines excited near the first IP.[7] The high density of Rydberg states in this region favors the existence of electronic couplings that may explain the observed ultrafast IC. Conical intersections between the optically active SE state and the Rydberg states likely play a crucial role in the electronic relaxation.

At the three explored wavelengths, the transients observed in the fragment channel have an additional lifetime in the picosecond time scale, τ_2. In the model proposed (Figure 9), this lifetime is associated with the subsequent relaxation of Rydberg states populated from the SE state. The absence of the picosecond lifetime in the parent ion channel suggests that the molecule undergoes complete dissociation when probed from the populated Rydberg states. The dependence of the fragment ion signal with the probe intensity (Figure 6) supports this interpretation. The larger number of photons absorbed to yield the fragment at long times reveals the transfer to the ion of the vibrational energy gained in the electronic relaxation, which results in the formation of ionic fragments. The origin of the picosecond lifetime is plausibly explained by fragmentation of the neutral molecule. In this picture, the vibrational energy released during the electronic IC will flow into reactive modes leading to fragmentation. The process is presumably controlled by IVR, whose lifetime is commonly accepted to be in the picosecond time scale. Eventually, the neutral products of the reaction might be ionized by the probe laser, though no evidence of this ionization has been found in the mass spectra. A similar relaxation mechanism has been reported to be responsible for the photochemical reactivity of tertiary amines excited near the IP.[7]

It is worth noting that the creation of SE states seems to be an efficient and common process in polyatomic molecules excited, via resonant or nonresonant multiphoton absorption, in a few electronvolts over the first IP. A similar ultrafast relaxation dynamics has been observed in phenol,[5] cyclohexadien,[6] and amine derivatives.[7] NPH and AMN prepared in SE states have a similar behavior regardless of the characteristic electronic configuration introduced by the amino group substituent. It is likely that the $\pi-\pi^*$ character of the first excitation step common to both molecules drives the system toward a final configuration built up mostly of excited π electrons. In addition, even if excitations of the nonbonding n nitrogen electrons were involved in the final configuration, the electronic coupling to Rydberg states would proceed through a similar ultrafast relaxation. Indeed, ultrafast IC is known to be a common process in aromatic molecules when pumped over the first electronic excited state.[23] In the same way, the molecule shows similar relaxation dynamics when excited through S_1 or S_2 states with a variable energy excess over the first IP; in fact, only a minor increase in the rate of the femtosecond constant with the excitation energy is observed. This result suggests that even if the configurations reached in the studied interval of energy were different, ultrafast coupling to Rydberg levels via conventional IC or conical intersections is the primary relaxation mechanism.

Direct Ionization, Autoionization, and Other Interfering Processes. It has been shown that the production and relaxation of the SE states occurs simultaneously with other photophysical processes. In some cases, they contribute to the decays, contaminating the dynamics of the states of interest. Prompt ionization is associated with the fraction of molecules that couples to the continuum following the absorption of the second pump photon and competes with the formation of the SE state. On the other hand, autoionization is produced by former SE

molecules that decay to Rydberg autoionizing states. Although the transients of the parent and fragment ions do not reflect the dynamics of these processes, they contribute indirectly to the decays. The sum of prompt ionized and autoionized molecules appears in the parent ion transients as a constant offset, whose magnitude can be observed in part d of Figure 3, part b of Figure 7, and parts a−c of Figure 8, where the vertical scale refers to the absolute zero ion current. The background may also contain ions created by absorption of a third pump photon from the SE state, although this contribution is expected to be small because of the pump laser low intensity.

Prompt and autoionized ions (not necessarily with the same distribution of electronic and vibrational states) reside in the acceleration region of the TOF spectrometer during a long enough time to absorb probe photons, yielding fragments that appear in their own mass channels. This effect generates a background at positive delay times observed in the transients of both $C_{10}H_7^+$ and AMN^+-28 fragments. The rising slope of the background should match the rate of autoinization. The fact that no other lifetime is needed to fit the fragment transients implies a negligible autoionization contribution to the background or, alternatively, an autoionization process with a growth component very close to the SE state relaxation lifetime τ_1.

Fragmentation of prompt ionized and autoionized molecules induced by the probe laser also accounts for the depletion observed in the baseline of the parent ion decays at positive delay times (cf. part b of Figure 7). In the above statement, it has been necessary to check that the probe beam does not induce any parent or fragment ion by itself, or when preceding the pump.

Fragmentation of parent ions by multiphoton absorption of the probe laser might also include the cation dynamics. Examples are provided in the study of charge transfer processes by Lehr et al.[24] and more recently in the work on ionic resonances by Pearson et al.,[25] where they demonstrate how probe dissociation may be used to resolve the ion wave packet oscillations. Ion dynamics may be particularly important in NPH^+, where the D_2, D_1, and D_0 states have been extensively studied and are known to be strongly coupled.[26,27] IC in the femtosecond time scale has been observed in the D_2 state of the cation.[28] We believe that the cation dynamics is not present in our fragment measurements, or at least its little contribution does not affect the information derived for the neutral species. The fact that at the different excitation wavelengths, which yield ions in different electronic and vibrational states, the observed constants in the fragment channels are very similar allows one to exclude large ionic contributions.

Concluding Remarks

Two-photon resonant excitation of NPH and AMN via S_1/S_2 intermediate states yields SE states with energies in the 7.45−9.3 eV range. Although NPH S_1 and S_2 states correlate with the D_0 and D_1 ion states, the formation of neutral SE states efficiently competes with the ionization channels. The relaxation dynamics of the SE states has been investigated with femtosecond resolution. The sensible tuning of pump and probe laser intensities permits the separation of the dynamics of the SE states from that of S_1/S_2 intermediate excited states.

The first stage of the relaxation involves the ultrafast IC to Rydberg states. Probing these states results in the formation of ionic fragments when the electronic energy funneled to the vibrational modes is transferred to the ion. A second picosecond lifetime only observable in the fragment channels is associated with the fragmentation of the neutral species driven by IVR. The study demonstrates for molecules excited over the IP the significance of a relaxation pathway that takes place along excited states of the neutral species alternatively to ionization channels.

Acknowledgment. This work has been partially funded by Spanish MEC under Grants CTQ2003-0510 and Consolider SAUUL CSD2007-00013, by the Basque Government (BG) through a Complimentary Action, and by UPV-EHU Consolidated Group Program. The experimental work was carried out at the Laser Facility of the UPV/EHU SGIker, supported by FEDER, MCYT, and BG. A.L. acknowledges MEC for a Ramón y Cajal contract.

References and Notes

(1) (a) Platzman, R. L. *Vortex* **1962**, *23*, 372. (b) Platzman, R. L. *Radiat. Res.* **1962**, *16*, 419.
(2) (a) Softley, T. P. *Int. Rev. Phys. Chem.* **2004**, *23*, 1. (b) Hatano, Y. *Radiat. Phys. Chem.* **2003**, *67*, 187. (c) Hatano, Y. *Phys. Rep.* **1999**, *313*, 110. (d) Merkt, F. *Annu. Rev. Phys. Chem.* **1997**, *48*, 675. (e) Pratt, S. T. *Rep. Prog. Phys.* **1995**, *58*, 82.
(3) (a) Müller-Dethlefs, K.; Schlag, E. W. *Annu. Rev. Phys. Chem.* **1991**, *42*, 109. (b) Cockett, M. C. R. *Chem. Soc. Rev.* **2005**, *34*, 935.
(4) (a) Pinnaduwage, L. A.; Zhu, Y. *Chem. Phys. Lett.* **1997**, *277*, 147. (b) Pinnaduwage, L. A.; Zhu, Y. *J. Chem. Phys.* **1998**, *108*, 6633.
(5) (a) Schick, C. P.; Weber, P. M. *J. Phys. Chem. A* **2001**, *105*, 3725. (b) Schick, C. P.; Weber, P. M. *J. Phys. Chem. A* **2001**, *105*, 3735.
(6) Cheng, W.; Evans, C. L.; kuthirummal, N.; Weber, P. M. *Chem. Phys. Lett.* **2001**, *349*, 405.
(7) Sølling, T. I.; Kötting, C.; Zewail, A. H. *J. Phys. Chem. A* **2003**, *107*, 10872.
(8) (a) Blanchet, V.; Zgierski, M. Z.; Stolow, A. *J. Chem. Phys.* **2001**, *114*, 1194. (b) Scmitt, M.; Lochbrunner, S.; Shaffer, J. P.; Larsen, J. J.; Zgierski, M. Z.; Stolow, A. *J. Chem. Phys.* **2001**, *114*, 1206.
(9) Montero, R.; Longarte, A.; Martínez, R.; Castaño, F. Manuscript in preparation.
(10) Dantus, M.; Janssen, M. H. M.; Zewail, A. H. *Chem. Phys. Lett.* **1991**, *181*, 281.
(11) Pedersen, S.; Zewail, A. H. *Mol. Phys.* **1996**, *89*, 1455.
(12) *Matemática 6.0*; Wolfram Research Inc.: Champaign, Illinois, 2007.
(13) Montero, R.; Longarte, A.; Martínez, R.; Castaño, F. Manuscript in preparation.
(14) (a) Trushin, S. A.; Fuβ, W.; Schmid, W. E. *J. Phys. B* **2004**, *37*, 3987. (b) Fuβ, W.; Schmid, W. E.; Trushin, S. A. *J. Chem. Phys.* **2000**, *112*, 8347.
(15) Pedersen, S.; Baumert, T.; Zewail, A. H. *J. Phys. Chem.* **1993**, *97*, 12460.
(16) Rubio, M.; Merchán, M.; Ortí, E.; Roos, B. O. *Chem. Phys.* **1994**, *179*, 395.
(17) Pino, T.; Boudin, N.; Bréchignac, P. *J. Chem. Phys.* **1999**, *111*, 7337.
(18) Berden, G.; Meerts, W. L.; Plusquellic, D. F.; Fujita, I.; Pratt, W. *J. Chem. Phys.* **1996**, *104*, 3935.
(19) Lahmani, F.; Zehnacker-Rentien, A.; Coudert, L. H.; Zachariasse, K. A. *J. Phys. Chem. A* **2003**, *107*, 7364.
(20) Jiang, S.; Levy, D. H. *J. Phys. Chem. A* **2002**, *106*, 8590.
(21) Jochims, H. W.; Rasekh, H.; Rühl, E.; Baumgärtel, H.; Leach, S. *Chem. Phys.* **1992**, *168*, 159.
(22) Kuthirummal, N.; Weber, P. M. *J. Mol. Struct.* **2006**, *787*, 163.
(23) Shih-Huang, L.; Kuo-Chun, T.; I-Chia, C.; Schmitt, M.; Shaffer, J. P.; Schultz, T.; Underwood, J. G.; Zgierski, M. Z.; Stolow, A. *J. Phys. Chem.* **2002**, *106*, 8979.
(24) Lehr, L.; Horneff, T.; Weinkauf, R.; Schlag, E. W *J. Phys. Chem. A* **2005**, *109*, 8074.
(25) Pearson, B. J.; Nichols, S. R.; Weinacht, T. *J. Chem. Phys.* **2007**, *127*, 131101.
(26) Cockett, M. C. R.; Ozeki, H.; Okuyama, K.; Kimura, K *J. Chem. Phys.* **1993**, *98*, 7763.
(27) Katherine, F. H.; Boggio-Pasqua, M.; Bearpark, M. J.; Robb, M. A. *J. Phys. Chem. A* **2006**, *110*, 13591.
(28) Zhao, L.; Lian, R.; Shkrob, I. A.; Crowell, R. A.; Pommeret, S.; Chronister, E. L.; Liu, A. D.; Trifunac, A. D. *J. Phys. Chem. A* **2004**, *108*, 25.

JP8056064